Effect of the Air-Jet and the False-Twist Texturing Processes on the Stress-Relaxation of Polyamide 6.6 Yarns

A. M. Manich,[1] J. Maíllo,[2] D. Cayuela,[3] J. Gacén,[3] M. D. de Castellar,[1] M Ussman[4]

[1]*Ecotecnologies Department, CSIC, Barcelona (Spain)*
[2]*Departament d'Enginyeria Tèxtil i Paperera, UPC, Terrassa (Spain)*
[3]*Intexter, UPC, Terrassa (Spain)*
[4]*Universidade da Beira Interior, Covilhã, Portugal*

Received 15 December 2006; accepted 6 March 2007
DOI 10.1002/app.26438
Published online 8 May 2007 in Wiley InterScience (www.interscience.wiley.com).

ABSTRACT: Polyamide 6.6 multifilament yarns were converted to crimped fibers by texturing to simulate the properties of natural staple fiber yarns for textile applications. Texturing is carried out by mechanical stresses (turbulences or twisting) under thermal or hydrothermal conditions which affect the fine structure of the fiber. Two polyamide yarns with the same linear density but composed of filaments of different fineness were textured by the False-Twist (thermal) and the Air-Jet (hydrothermal) procedures. The influence of texturing and filament fineness on the relaxation behavior of the yarns was studied. © 2007 Wiley Periodicals, Inc. J Appl Polym Sci 105: 2482–2487, 2007

Key words: polyamide 6.6; texturing; air-jet; false-twist; filament fineness; stress-relaxation; modeling

INTRODUCTION

All polyamide fibers consist of linear polymers with molecules that are oriented along the fiber axis to a greater or lesser extent. The properties of the fiber are determined by the molecular structure and the molecular organization. The fiber structure may be viewed at three different levels: (1) the chemical structure, (2) the fine structure which is concerned with the way in which the polymer molecules are arranged within the fiber and (3) the gross morphology which can be assessed by its appearance under an optical microscope. The fiber is produced by extrusion of the molten polymer, resulting in some skin-core differentiation owing to rapid cooling at the surface of the fiber. Subsequent processes, which involve heating the fiber and also drawing, will allow some further rearrangement of the molecules and increased crystallinity. Polyamide fibers are often considered to be ~50% crystalline. The use of the term crystalline implies that there are discrete crystalline and amorphous regions but it seems unlikely that the morphological structure of nylons consist entirely of a simple two-phase model in which perfectly ordered crystallites exist in equilibrium with amorphous regions. The fiber may also be regarded as a *para*-crystalline form in which all deviations from the ideal crystal structure are attributed to defects and distortions of the lattice.

When polyamide fibers are drawn, the polymer molecules and the crystalline aggregates will be oriented in the direction of draw; crystallinity is likely to develop further in amorphous or partly crystalline material. The orientation will depend on the rate of drawing and temperature.[1,2] According to Oudet the amorphous phase is made up of the amorphous oriented and the amorphous isotropic regions, which link the macro fibrils and the micro fibrils, respectively.[3]

Texturing is the conversion of flat (straight) filament yarn to crimped fibers to simulate the properties of natural staple yarns of increased bulk with the benefits of thermal insulation, cover, softness and fullness, and moisture transport. In false twist texturing, the multifilament bundle is cold twisted by running the yarn over the edge of a stack of nine rotating discs on three centers in an equilateral triangle. The yarn runs through the center of the triangle and over the edge of each disc. Twisted yarn passes the heater where it is heat plasticized and twists are heat set in a dry atmosphere close to its melting point. The yarn is cooled in the area between the heater and the spindle and untwisted after passing the spindle. Heat-set twists impart crimp, bulk and elasticity to the yarn.[4] In air jet texturing, the multifilament bundle is fed into a jet, where it interacts with supersonic, turbulent, nonuniform air flow. Water is sprayed immediately before the jet to lubri-

Correspondence to: A. M. Manich (ambeco@cid.csic.es).
Contract grant sponsor: M. E. C. Dirección general de Investigación; contract grant numbers: MAT2004-04, 981-C03-03.

cate the yarn. Upon emerging from the jet, the filaments bend into bows and arcs, forming filament loops on the surface of the yarn. These loops are locked in the resulting textured yarn assembly due to intermingling of the filaments. In air-jet texturing, multifilaments are textured in a humid hot atmosphere.[5] This kind of dry and humid thermal post treatment modifies the fine structure of the fiber in three ways: (1) it increases crystallinity by a secondary recrystallization, (2) it rearranges preferentially macro fibrils near the surface, enhancing the skin-core differentiation effect and, (3) it enables the polymer to form larger crystals which stabilize the fiber in the deformed state. All these effects will influence the stress-relaxation behavior of the yarns.

We previously studied the influence of texturing on the thermal stability of PA 6.6 yarns by thermal analysis. Variations in crystallinity were measured by DSC and TMA (Thermo Mechanical Analysis), enabling us to measure the broadening of the glass transition effect, the dimensional stabilization and the shrinkage forces developed by texturing. It was observed that texturing favors a partial recrystallization of the amorphous component, increasing fiber crystallinity especially in the thicker filaments.[6] In this work we focus our attention on the stress-relaxation of the yarns when these are stretched at a fixed extension. In these experiments the external geometry of the specimen remains unchanged throughout the test.[7]

Spring and dashpot elements are frequently used to allow a mathematical analysis of stress relaxation. A spring element behaves exactly like a metal spring, stretching instantly when stress is applied, maintaining the stress indefinitely, and returning to its original dimension instantly when stress is removed. In a dashpot under stress, the plunger moves through the fluid at a rate that is proportional to the stress. There is no recovery in the dashpot on removing the stress. A spring of E_m modulus and a dashpot of η_m viscosity in series are known as the Maxwell element[8] [Fig. 1(a)]. The initial stress σ_i will decrease with time at a rate characterized by the relaxation time τ, at which the stress of the Maxwell element $\sigma(\tau)$ will be 36.8% of the initial stress σ_i.[9]

The stress-relaxation will be the result of the different relaxation processes occurring at each level of the fiber structural hierarchy. Komanowsky et al. and Attenburrow et al.[10,11] highlight the stress relaxation processes occurring at different structural levels of leather. Consequently, it seems reasonable to use the generalized Maxwell model [Fig. 1(b)] to account for the stress relaxation of the fiber. To calculate the discrete spectrum of relaxation times to match the different levels of the structural hierarchy of the fiber (skin-core differentiation, macro fibrils, micro fibrils), the researcher determines the values

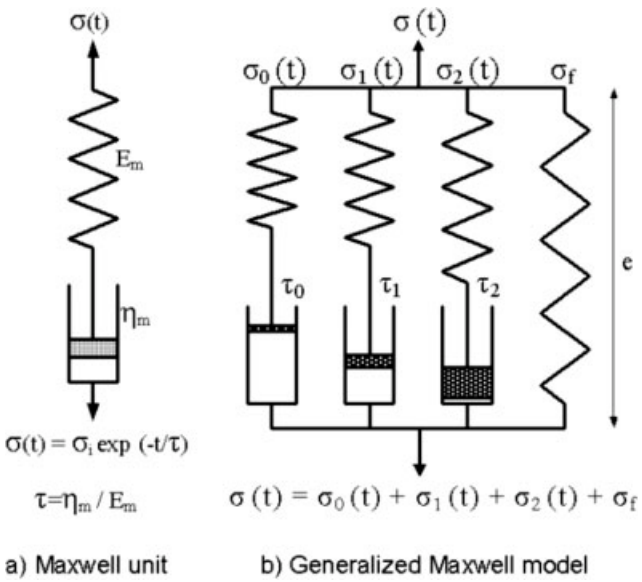

Figure 1 (a) Maxwell unit, (b) Generalized Maxwell model to account for the stress relaxation of Poliamide 6.6 multifilaments.

of relaxation times *a priori* according to different criteria. Vitkauskas[12] suggests the relation $\tau_i = 10^i\ \tau_0$, where τ_0 is the minimal value and the values of relaxation times differ from each other exactly by one order of magnitude.

The generalized Maxwell model presented in this work [Fig. 1(b)] consists of a set of three Maxwell units connected in parallel and a Hookean spring in parallel to represent the stress σ_f at the equilibrium. The strain e of the generalized model equals the strain of each element of the model and the stress $\sigma(t)$ of the generalized model is the sum of the partial stresses on each of the elements. The mathematical representation of the stress relaxation for such a model is given by the following equation:

$$\sigma(t) = \sigma_0\ \exp(-t/\tau_0) + \sigma_1\ \exp(-t/\tau_1) + \sigma_2\ \exp(-t/\tau_2) + \sigma_f \quad (1)$$

σ_0 being the high-rate relaxed stress at τ_0 relaxation time, σ_1 the medium-rate relaxed stress at τ_1 relaxation time, and σ_2 the low-rate relaxed stress at τ_2 relaxation time, σ_f would correspond to the nonrelaxed stress known also as the final stress or the stress at the equilibrium after relaxation. Values of relaxed and nonrelaxed stresses are expressed as reduced stress obtained by dividing the stress observed at time t by the initial stress σ_i expressed in %.

This study seeks to (1) demonstrate the suitability of the proposed model to account for the stress relaxation process of polyamide 6.6 yarns textured under thermal and hydro-thermal conditions; (2)

TABLE I
Sample Reference According to the Yarn Type and False-Twist FT and Air-Jet Texturing Procedure

Sample Ref.	Linear densities [dtex] × nr. filaments	Texturing procedure	Breaking stress		Breaking strain	
			[MPa]	CV[%]	[%]	CV[%]
B	1.27dtex × 68	Original	355.65	(4.49)	63.21	(5.57)
B1	(R 8.67 tex/68)	FT at 200°C	415.27	(3.70)	28.00	(8.10)
B2		FT at 210°C	372.21	(5.17)	27.77	(6.73)
B3		FT at 220°C	386.63	(3.56)	29.86	(7.27)
B4		FT at 230°C	408.47	(3.99)	26.81	(6.05)
C	1.27dtex × 68	Original	383.20	(6.00)	65.31	(20.70)
C1	(R 8.67 tex/68)	Air-Jet text	407.43	(4.07)	35.04	(15.15)
E	3.77dtex × 23	Original	395.11	(5.56)	68.00	(7.07)
E1	(R 8.67 tex/23)	FT at 200°C	591.14	(10.34)	33.78	(23.97)
E2		FT at 210°C	460.50	(6.45)	29.57	(11.65)
E3		FT at 220°C	501.17	(12.44)	32.81	(10.36)
E4		FT at 230°C	504.20	(12.14)	31.56	(26.78)
F	3.77dtex × 23	Original	380.23	(4.83)	58.87	(5.54)
F1	(R 8.67 tex/23)	Air-Jet text	410.24	(2.67)	30.13	(9.03)

Breaking stress and strain including the coefficients of variation in brackets.

show to which degree texturing conditions could affect the initial stress, the final stress and the high-rate, medium-rate and low rate relaxed stresses of polyamide 6.6 yarns to determine which structural level is the most affected by the texturing processes; and (3) to study the relationship between recrystallization and the initial and final stresses which are related to bonding formation by texturing and bonding breakdown by stress which induces stress relaxation.

Objective

The aim of this work is to study the effect of the texturing processes and conditions on the stress-relaxation of polyamide 6.6 yarns stretched 25% by measuring the relaxation of the stress along 180 s because variations of stress thereafter was quite negligible.[13] The influence of the filament fineness will also be considered.

EXPERIMENTAL

Materials

Experiments were done on 86.67 dtex polyamide 6.6 multifilament yarns from the same producer, made up of two different type of monofilaments: Thin filaments of 1.27 dtex in fineness resulting in a 1.27 dtex × 68 (R 8.67 tex/68) multifilament yarn and thick filaments of 3.77 dtex in fineness resulting in a 3.77 dtex × 23 (R 8.67 tex/23) multifilament yarn.

Both yarns were thermally treated by the False-Twist texturing procedure at 200, 210, 220, and 230°C and hydro thermally treated by the Air-Jet procedure. References which identify filament fineness and texturing conditions are shown in Table I.

METHODS

Tensile properties of the multifilaments

Ten specimens with gauge length of 100 mm were tested after being conditioned in a standard atmosphere for 48 h. Breaking stress [MPa] and strain [%] were determined on specimens subjected to tensile testing at 60%/min according to the ASTM D 2101 Standard.[14]

Stress relaxation test

Five specimens with gauge length of 100 mm were tested after being conditioned in a standard atmosphere for 48 h. Specimens were subjected to 25% of straining because it was the maximum level of stretching all yarns were able to withstand without breaking. Yarns were strained at 60%/min with pretension of 20 MPa in the MT-LQ dynamometer. The average of the initial stress σ_i and stresses at 1, 2, 3, 4, 5, 6, 7, 8, 10, 12, 14, 16, 18, 20, 25, 30, 35, 40, 45, 50, 60, 70, 80, 100, 120, 140, 160, and 180 s were recorded.

Fitting the stress relaxation model

The relaxation times were preselected $\tau_0 = 1$ s, $\tau_1 = 10$ s, and $\tau_2 = 100$ s to differ between them in one order of magnitude and to be placed into the length of time of the stress-relaxation test according to Vitkauskas's conditions.[12] Based on the preselected relaxation times, the multiple regression analysis[15,16] was used to obtain the estimators of high-rate σ_0, medium-rate σ_1, low-rate σ_2 relaxed stresses, and σ_f the nonrelaxed or final stress. The determination coefficients of the all fitted multiple regression equations ranged from 99.76 to 99.95%. All the terms

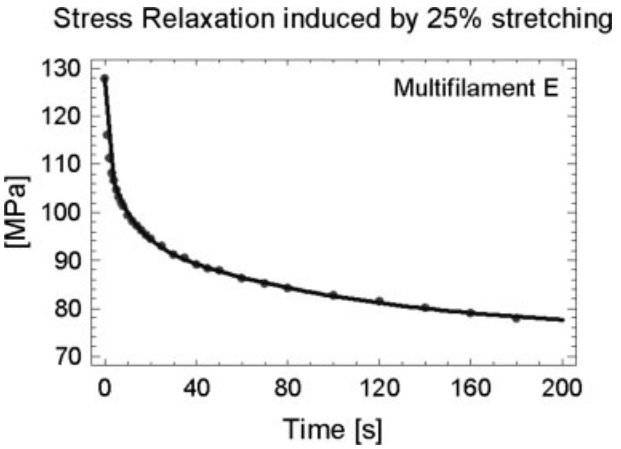

Figure 2 Stress relaxation of multifilament E stretched 25% and generalized Maxwell model fit to explain the relaxation behavior.

were highly significant, which explains that relaxation is produced as a consequence of three relaxation processes occurring in parallel (cfr. Fig. 2). Values of reduced stress obtained by dividing the stress observed at time t by the initial stress σ_i expressed in % were used.

RESULTS AND DISCUSSION

Mean values of stress and strain at breaking with the corresponding coefficients of variation are given in Table I. The results of fitting the stress-relaxation model (cfr. eq. 1) are shown in Table II. The initial stress σ_i at 25% of stretching, the stress at the end of the relaxation test σ_{3min}, the fitted final stress σ_f after relaxation, the high-rate σ_0, the medium-rate σ_1 and the low-rate σ_2 relaxed stresses in % of the initial stress at relaxation times $\tau_0 = 1$ s, $\tau_1 = 10$ s and $\tau_2 = 100$ s respectively, values of crystallinity K,[6] the determination coefficient R^2 of the fitted equations and the cumulated relaxed stresses at high and medium rates $\sigma_0 + \sigma_1$ are included.

Stress and bonding formation

Texturing increases both the initial and final stresses of yarns stretched 25% owing to bond formation. Bond formation includes processes analogous to formation of larger crystals, recrystallization at the expense of the amorphous phase, formation of hydrogen bonds between adjacent chains or even new chemical links at the amorphous oriented and isotropic phases.

The Air-Jet texturing of thicker filaments causes both the highest increase in the initial stress and the highest relaxation of stress, which can be explained by the highest formation of secondary bonds of low energy induced by this hydrothermal process. Similar behavior was observed in thin filaments. The recrystallization induced by this process was lower than that produced by the thermal process of False-twist texturing.

The effect of the False-Twist texturing process on the initial stress depends on the filament fineness. Thin filaments reached the highest initial stress (maximum bonding formation) at 200°C, which remains stable despite increasing the temperature up to 230°C. Thick filaments show lower values of initial stress which ascends when increasing temperature from 200 to 230°C. Thin filaments showed lower relaxation than the thicker ones, which means that in addition to the higher level of bonding formation

TABLE II
Values of Crystallinity K [Ref. 6], and Values of the Initial Stress σ_i in [MPa] and Final Stress after 3 min of Relaxation σ_{3min} at 25% of Stretching, and Those of the Final Stress σ_f and Relaxed Stresses at 1 s σ_0, 10 s σ_1, and 100 s σ_2 as % of the Initial Stress Along the Relaxation Test, the Determination Coefficient R^2 and the Cumulated Relaxed Stresses at 1 s and 10 s $\sigma_0 + \sigma_1$

Ref.	K [%]	σ_i [MPa]	σ_{3min} [%σ_i]	σ_f [%σ_i]	σ_0 [%σ_i]	σ_1 [%σ_i]	σ_2 [%σ_i]	R^2 [%]	$\sigma_0 + \sigma_1$ [%σ_i]
B	33.0	123.2	67.68	62.79	10.96	15.76	10.48	99.76	26.72
B1	36.8	250.2	76.41	75.12	7.96	9.61	7.31	99.93	17.57
B2	37.9	235.6	76.43	75.69	8.00	9.63	6.67	99.93	17.63
B3	38.5	258.5	77.04	73.93	7.85	10.19	8.03	99.85	18.04
B4	38.8	263.3	75.36	75.13	8.50	8.98	7.39	99.95	17.48
C	35.1	140.4	65.18	62.88	11.42	13.72	11.98	99.92	24.69
C1	37.6	250.1	71.74	69.26	9.17	8.08	13.49	99.86	17.25
E	35.9	127.8	60.93	58.47	12.36	12.58	16.59	99.95	24.94
E1	36.8	169.6	73.45	71.82	8.78	8.39	11.02	99.88	17.17
E2	38.0	188.4	75.22	73.23	9.06	8.31	9.40	99.89	17.37
E3	39.9	191.5	74.29	73.33	8.18	8.18	10.30	99.92	16.36
E4	41.0	224.0	74.98	72.34	8.27	7.90	11.49	99.94	16.17
F	35.2	136.0	62.70	60.13	12.24	13.05	14.58	99.90	25.29
F1	37.0	283.1	71.36	69.53	11.32	7.82	11.32	99.88	19.14

they were stronger than bonds formed in thicker filaments.

Dry thermal treatment mainly promotes the formation of high energy bonds including the hydrogen bonds linking due to recrystallization which cannot easily be broken down by stress. As a consequence, the final stresses after relaxation of False-Twist textured yarns were higher than the final stress of the Air-Jet textured yarns.

Relaxation and bonding breakdown

Relaxation is probably caused by bond breakdown reactions owing to stress. The lower the energy barrier that separates the two states of stable equilibrium of the bond network, the higher the amount of breaking bonds. Although the amount of bond formation by texturing can be regarded as similar regardless of the texturing procedure, the energy barrier of the bonds produced by Air-Jet texturing seems to be lower than that of the bonds formed by False-Twist texturing.

We can attribute the high and the medium rate relaxed stresses to the breakdown of bonds in the amorphous oriented phase that links the macrofibrils that are mainly placed in the sheath of the filament, whereas the low rate relaxed stress could be ascribed to the breakdown of bonds in the amorphous isotropic phase that links the microfibrils that are mainly placed in the core of the filament.

False-Twist texturing promotes the formation of strong hydrogen bonds between the —CO NH— groups of adjacent chains in the amorphous oriented phase, favoring the formation of new polyamide crystals and increasing the skin-core differentiation of the filaments. However, owing to the difficulties of sorting out chains, crystallization will not be complete.[17] This results in a decrease in the high and medium relaxation stresses from 25 to 17% regardless of filament fineness. The increase in skin at the expense of the core is particularly relevant in the case of thin filaments where the low-rate relaxation stress decreases up to 6–8%, whereas for thick filaments it decreased up to 9–11%, approximately.

For thin filaments the formation of strong bonds in the sheath of filaments by the hydrothermal texturing process resembles that of the thermal texturing process for thin filaments (high and medium rate relaxation of 17.25%). For the thicker ones the formation of strong bonds at the sheath was lower (high and medium rate relaxation of 19.14%) at expenses of the formation of this kind of strong bonds at the core (low rate relaxation of 11.32%). Lower formation of strong bonds at the core of thin filaments by hydrothermal texturing is observed (low rate relaxation of 13.49%). The hydrothermal texturing treatment supply water that, when absorbed, promotes swelling of polymer increasing the distance between the groups —CO NH— of adjacent chains, some of them linked by strong hydrogen bonds. Then it is possible to place a water molecule by forming the linkage —CO—HOH—NH— which is not as strong as the first —CO—NH— linkage.[3]

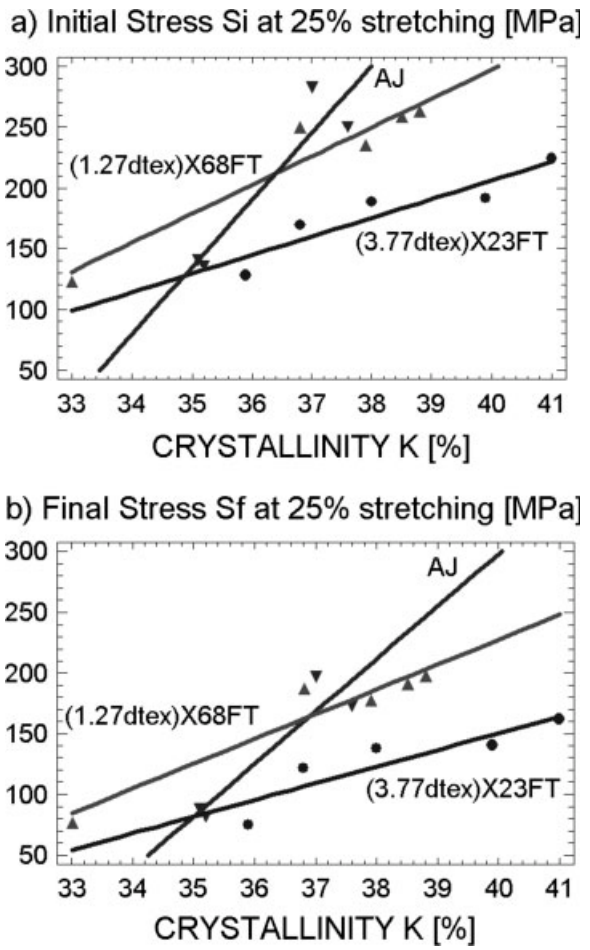

Figure 3 Regression lines between (a) Crystallinity and Initial stress, and (b) Crystallinity and final stress (after relaxation) at 25% stretching of False-Twist textured thick filaments (3.77dtex ×23 FT), False-Twist textured thin filaments (1.27dtex ×68 FT) and Air Jet textured multifilaments AJ regardless of their fineness.

Bond formation and crystallinity

Figure 3a shows the relationship between crystallinity and the initial stress and Figure 3b the relationship between crystallinity and final stress after relaxation. The former reflects the connection between the bonding formed by texturing and crystallinity; the latter highlights the proportionality between strong bonds that remain after relaxation and crystallinity. The comparison between the regression lines in Figure 3[18] shows the regression lines relating the initial stress versus crystallinity

and the final stress versus crystallinity. Both regression lines are parallel for false twist textured thick filaments (slope = 14.53 MPa/%), false-twist textured thin filaments (slope = 22.08 MPa/%) and air-jet textured filaments regardless their fineness (slope = 67.38 MPa/%). By comparing the slope values it may be concluded that in False-Twist texturing the relationship between bonding formation and recrystallization is 1.5 times higher in thin filaments than in the thicker ones, which suggests that bonding formation (and recrystallization) is gradually produced from the sheath to the core of the filaments. By comparing the slope of the Air-Jet texturing filaments and the slopes of the False-Twist texturing filaments, the relationship between bonding formation and recrystallization of these processes is between three and four times higher, which suggests that bonding formation is higher in Air-Jet texturing although recrystallization is lower.

The difference between the intercepts of the regression of initial stress versus crystallinity and final stress versus crystallinity will represent the amount of stress that is relaxed due to the breakage of the weaker bonds. The stress relaxed by bonding breakage of False-Twist textured filaments was 52.88 MPa for thick filaments, 59.64 MPa for thin filaments, and 67.38 MPa for the Air-Jet textured filaments. Thermal treatments favor higher recrystallization and lower bonding between adjacent chains, whereas hydrothermal treatments favor higher bonding between adjacent chains despite its small effect on recrystallization.

CONCLUSIONS

Texturing increases both the initial and the final stress after relaxation of the polyamide 6.6 yarns when stretched 25% due to bond formation.

The Air-Jet texturing (hydrothermal treatment) causes the highest bonding formation and the highest relaxation (breakage of low energy bonds) at the expense of the lower increase in recrystallization.

The False-Twist texturing (dry thermal treatment) promotes the formation of high energy bonds favoring recrystallization, which cannot be easily broken by stress.

The False-Twist texturing favors the formation of strong bonds in the amorphous oriented phase, increasing the skin-core differentiation of filaments that are relevant in the case of thin filaments.

The proportionality between bonding formation measured by stress and crystallinity is 14.53 MPa/% for thick False-Twist textured filaments, 22.08 MPa/% for thin False-Twist textured filaments and 67.38 MPa/% for Air-Jet textured filaments, which suggests that the effect of False-Twist texturing occurs gradually from the sheath to the core of the filament, whereas the effect of the Air-Jet texturing reaches the core of the filament without difficulty.

The stress relaxed by bonding breakage is in accordance with the above conclusion. The lowest relaxation was observed in thick False-Twist textured filaments followed by thin False-Twist textured filaments and the Air-Jet textured showed the highest relaxation.

The authors recognize the contribution of the CSIC/GRICES 2005PT0051 Project helping the elaboration of the article, and they are also grateful to Ms. R Mateu, A Lopez, and C Martínez for their contribution to the experimental work and to Mr. George von Knorring for his technical support.

References

1. McIntyre, J. E. Synthetic Fibres: Nylon, Polyester, Acrylic, Polyolefin; Woodhead Publishing, CRC Press: Cambridge, 2005.
2. Hearle, J. W. S. J Appl Polym Sci Appl Polymer Symp 1991, 47, 1.
3. Marcellan, A. Microstructures, Micromecanismes et Comportement a Rupture de Fibres PA 66, PhD Thesis, Ecole National Superiore des Mines de Paris, B.P. 87, 91003 Evry Cedex 2003; p 12.
4. Foster, P. W.; Greenwood, K.; Jeetah, R.; Mukhopadhyay, S. K. J Text Inst 1992, 83, 414.
5. Hearle, J. W. S.; Hollick, L.; Wilson, D. K.; Yarn Texturing Technology, Woodhead Publishing: England, 2001.
6. Manich, A. M.; Maillo, J.; Cayuela, D.; Carilla, J.; Ussman, M.; Gacen, J. J. Therm Anal Calorim, to appear.
7. Meredith, R. The Mechanical Properties of Textile Fibres, North-Holland: Amsterdam 1956; Chapter 3, p 39.
8. Ward, I. M.; Hadley, D. W. An Introduction to the Mechanical Properties of Solid Polymers, Wiley: Chichester, 1983.
9. Manich, A. In Modelización reológica de fluidos alimentarios, PhD Thesis, Technical University of Catalonia UPC, Fluid Mechanics Department, Barcelona 1990, p 42.
10. Komanowsky, M.; Cooke, P. H.; Damert, W. C.; Kronick P. L.; McClintick, M. D. J Am Leath Chem Assoc 1995, 90, 243.
11. Attenburrow, G. E.; Covington, A. D.; Jeyapalina, S. In Modelling the Stress Relaxation Behaviour of Wet Leather, XXVII IULTCS Congress Proceedings, Cancún (Mexico), 2003.
12. Vitkauskas, A. Medziagotyra J Mater Sci 1996, 2, 65.
13. Nachane, R. P.; Hussain, G. F. S.; Patel, G. S.; Krishna Iyer K. R. J Appl Polym Sci 1986, 31, 1101.
14. Standard Test Method ASTM D 2101 Tensile Properties of Single Man-Made Textile Fibres taken from Yarns and Tows, 1979.
15. STATGRAPHICS Plus Statistical Software. Manugistics, Inc. 2115 East Jefferson Street, Rockville, Maryland 20852, USA
16. Draper, N. R.; Smith, H. In Applied Regression Analysis, 2nd ed.; Wiley: New York, 1981.
17. Morton, W. E.; Hearle, J. W. S. In Physical Properties of Textile Fibres, The Textile Institute: Manchester, 1986; p 61.
18. Mead, R., Curnow, R. N., Hasted, A. M. In Statistical Methods in Agriculture and Experimental Biology, 3rd ed.; Chapman & Hall/CRC: Boca Raton, FL, 2003; p 245.